ADVANCES IN VETERINARY SURGERY

Advances In Equine Upper Respiratory Surgery

JAN HAWKINS

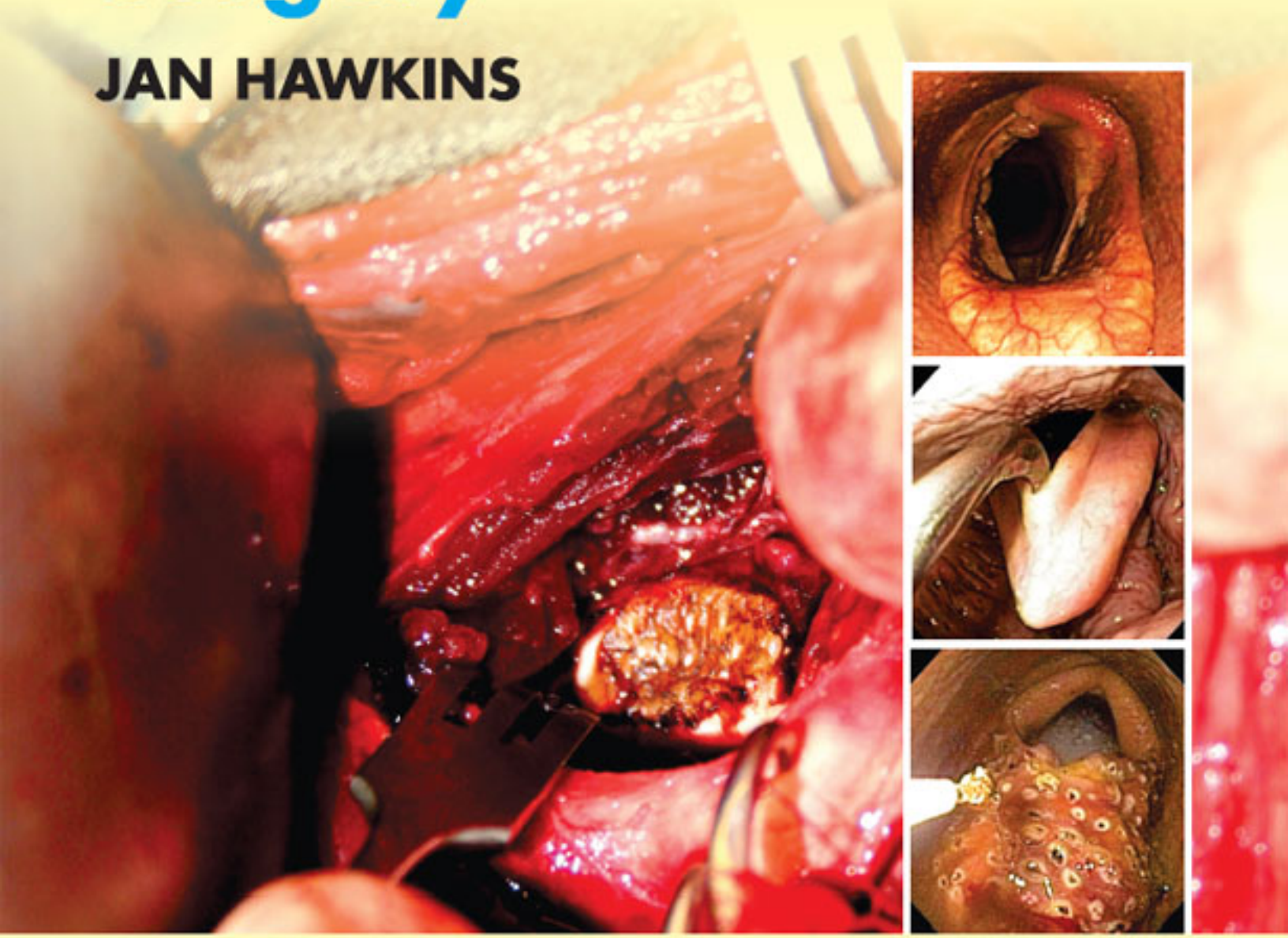

ACVS FOUNDATION

WILEY Blackwell

Advances in

Equine Upper Respiratory Surgery

Edited by

Jan Hawkins, DVM, DACVS
Department of Veterinary Clinical Sciences
Purdue University
Indiana, USA

WILEY Blackwell

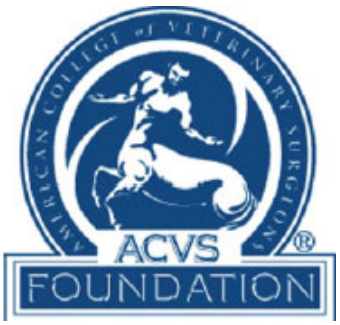
AMERICAN COLLEGE of VETERINARY SURGEONS
ACVS
FOUNDATION

This edition first published 2015 © 2015 by ACVS Foundation.

Editorial offices: 1606 Golden Aspen Drive, Suites 103 and 104, Ames, Iowa 50014-8300, USA
The Atrium, Southern Gate, Chichester, West Sussex, PO19 8SQ, UK
9600 Garsington Road, Oxford, OX4 2DQ, UK

For details of our global editorial offices, for customer services and for information about how to apply for permission to reuse the copyright material in this book please see our website at www.wiley.com/wiley-blackwell.

This work is a co-publication between the American College of Veterinary Surgeons Foundation and Wiley-Blackwell.

Library of Congress Cataloging-in-Publication Data

Advances in equine upper respiratory surgery / editor, Jan Hawkins.
p.; cm.
Includes index.
Summary: Advances in equine upper Respiratory surgery is a comprehensive, up-to-date
reference on surgical techniques in the upper respiratory tract in the horse, presenting theory and background as well as detailed procedures information.
ISBN 978-0-470-95960-2 (cloth)
I. Hawkins, Jan, editor.
[DNLM: 1. Horse Diseases–surgery. 2. Respiratory Tract Diseases–veterinary. 3. Respiratory Tract Diseases–surgery. 4. Surgery, Veterinary–methods. 5. Surgical Procedures, Operative–veterinary. SF 959.R47]
SF959.R47
636.1′0897542–dc23

2014022277

A catalogue record for this book is available from the British Library.

Wiley also publishes its books in a variety of electronic formats. Some content that appears in print may not be available in electronic books.

Contents

List of Tables

List of Illustrations

laryngoplasty. The hemostat in the photograph is grasping the knots of the suture material.

Figure 9.5 (a) Intraoperative photograph of right arytenoid abduction following repeat laryngoplasty. (b) Endoscopic photograph 1 day following right repeat laryngoplasty. (c) Endoscopic photograph 3 days following right repeat laryngoplasty. Note complete loss of abduction. This horse was subsequently treated with partial arytenoidectomy.

Chapter 10

Figure 10.1 A horse with dysphagia following prosthetic laryngoplasty. Note moderate abduction of the left arytenoid cartilage.

Figure 10.2 Feed material at the nares in a horse with clinical signs of dysphagia post prosthetic laryngoplasty.

Figure 10.3 Endoscopic photograph of horse with aspiration of feed material following prosthetic laryngoplasty.

Figure 10.4 Intraoperative photograph depicting removal of prosthetic suture material in a horse with postoperative dysphagia. No effort is made to transect adhesions associated with the prosthetic suture material.

Figure 10.5 (a) Preoperative endoscopic photograph and (b) Postoperative endoscopic photograph following prosthetic suture removal in a horse experiencing postoperative dysphagia. Also note the minimal loss of abduction. This also had laser ablation of the cricoarytenoid joint performed at the time of initial prosthetic laryngoplasty.

Chapter 13

Figure 13.1 Dorsal plane short tau inversion recovery turbo spin echo magnetic resonance image at the level of the cricothyroid articulation. The left side of the horse is to the right side of the image. The asterisk (*) indicates the normal left cricoid articular process and the white arrowhead indicates the normal caudal cornu of the left thyroid cartilage which forms the normal left cricothyroid articulation. The right side of the thyroid and cricoid cartilages do not articulate. The caudal cornu of the right thyroid cartilage lamina and the right cricoid articular process are absent. There is an abnormal gap between the cricoid and thyroid cartilages on the right. TC, thyroid cartilage; AC, arytenoid cartilage; CC, cricoid cartilage. Reprinted from Garrett et al. (2009) with permission from Wiley-Blackwell.

Figure 13.2 (a) Longitudinal ultrasound image of a normal larynx at the mid portion of the arytenoid cartilage. Cranial is to the left of the image. The cricoarytenoideus lateralis muscle is positioned in its normal location deep to the thyroid cartilage. The caudal cornu of the thyroid cartilage (*) is imaged close to its articulation with the cricoid cartilage. (b) Longitudinal image of the right side of the larynx of a horse with fourth branchial arch disorder at the midportion of the arytenoid cartilage. Cranial is to the left of the image. The cricoarytenoideus lateralis muscle is positioned between the thyroid cartilage and the cricoid cartilage in an abnormal space (between arrows). The caudal aspect of the thyroid cartilage (*) is abnormally shaped and does not articulate with the cricoid cartilage. TC, thyroid cartilage; CAL, cricoarytenoideus lateralis muscle; AC, arytenoid cartilage; CC, cricoid cartilage.

Reprinted from Garrett et al. (2009) with permission from Wiley-Blackwell.

Figure 13.3 Transverse proton density turbo spin echo magnetic resonance image at the level of the arytenoid cartilages. The left side of the horse is to the right side of the image. The lamina of the right side of the thyroid cartilage extends dorsal to the muscular process of the arytenoid cartilage (white arrow). The left side of the larynx is normal with the muscular process of the arytenoid extending dorsal to the thyroid lamina (black arrow). TC, thyroid cartilage; AC, arytenoid cartilage. Reprinted from Garrett et al. (2009) with permission from Wiley Blackwell.

Figure 13.4 (a) Transverse proton density turbo spin echo magnetic resonance image of a normal larynx at the level of the cricoid cartilage. The left side of the horse is to the right side of the image. (b) Transverse proton density turbo spin echo magnetic resonance image of a horse with fourth branchial arch disorder at the level of the cricoid cartilage. The left side of the horse is to the right side of the image. Note the widening and rotation to the right of the spine of the cricoid cartilage and subsequent abnormal positioning of the left and right cricoarytenoideus dorsalis muscles. The left cricopharyngeus muscle is present while the right cricopharyngeus muscle and cricoid articular process are absent. CAD, cricoarytenoideus dorsalis muscle; CP, cricopharyngeus muscle; CC, cricoid cartilage. Reprinted from Garrett et al. (2009) with permission from Wiley Blackwell.

Figure 13.5 Resting upper airway examination of a horse with fourth branchial arch abnormality. Note

the rostrally displaced position of the palatopharyngeal arch (black arrowheads).

Figure 13.6 Lateral–lateral radiograph of the pharyngeal and laryngeal region of a horse with fourth branchial arch abnormality. Rostral is to the left of the image. The rostrally displaced palatopharyngeal arch can be seen as a teardrop-shaped soft tissue opacity (black arrow). Air is present within the esophagus (white arrows).

Chapter 17

Figure 17.1 Resting videoendoscopic image of the pharynx of a horse with dorsal displacement of the soft palate.

Figure 17.2 Resting videoendoscopic image of the pharynx during nasal occlusion. Note the “flaccid” appearance of the epiglottis and soft palate instability.

Figure 17.3 Dorsal displacement of the soft palate. Note the ulcer (arrow) along the dorsal aspect of the caudal free edge.

Figure 17.4 Exercising images of spontaneous dorsal displacement of the soft palate. (a) Inspiration, (b–d) progressive upper airway obstruction of the soft palate during expiration.

Figure 17.5 (a, b) Progressive billowing of the soft palate dorsally.

Figure 17.6 (a–d) Axial deviation of the aryepiglottic immediately prior to dorsal displacement of the soft palate.

Figure 17.7 Exercising videoendoscopic images of the pharynx. (a) flaccid epiglottis, (b–d) progressive

loss of the normal subepiglottic position of the soft palate.

Figure 17.8 Concurrent epiglottic entrapment and persistent dorsal displacement of the soft palate. Entrapping aryepiglottic tissue (white arrow) is ventral to the soft palate (black arrow).

Chapter 18

Figure 18.1 Composite ultrasound images of the rostroventral (a, b) and midventral (c) acoustic windows of the throat region of a 4-year-old Standardbred gelding presenting with and upper respiratory noise during exercise. Images (a) and (b) depict the bony landmarks used to locate the basihyoid bone, beginning cranially in the transverse plane the lingual process (LP) and the base of the basihyoid bone (BH). Both can be identified by the hyperechoic surface and the strong acoustic shadow. Image (c) is obtained in a cranial (Cr) to caudal (Cd) direction, and demonstrates the characteristic slope of the base of the basihyoid bone, such that the depth of the basihyoid bone is different cranially (Cr) than caudally (Cd). For this reason, to ensure standardization of findings, it is recommended to assess basihyoid depth at the cranial aspect of the basihyoid bone, as the lingual process is merged with the base of the bone, as depicted in (b).

Chapter 19

Figure 19.1 Ventral midline incision centered over the caudal aspect of the cricoid cartilage. The hemostat marks the cricoid cartilage. Rostral is toward the left and caudal is toward the right of the photograph.

Figure 19.2 Gross postmortem photograph depicting isolation of the left sternothyroideus muscle. Note insertion of the sternothyroideus on the thyroid cartilage. Rostral is toward the left and caudal is toward the right of the photograph.

Figure 19.3 Gross postmortem photograph depicting clamping of the tendon of insertion of the sternothyroideus muscle and the muscle belly.

Figure 19.4 Gross postmortem photograph depicting transection of the tendon of insertion of the sternothyroideus muscle with Metzenbaum scissors.

Figure 19.5 Gross postmortem photograph depicting a laryngotomy incision through the cricothyroid ligament. Gelpi retractors are being used to open the cricothyroid space. Rostral is toward the left and caudal is toward the right.

Figure 19.6 Gross postmortem photograph depicting exposure of the caudal aspect of the soft palate. The thyroid cartilage and rostral aspect of the larynx have been removed. Note the characteristic V shape of the soft palate.

Figure 19.7 Gross postmortem photograph depicting grasping of the soft palate on the midline with straight sponge forceps and the incision of the soft palate on the left side with curved scissors.

Figure 19.8 Gross postmortem photograph depicting the two “tags” left behind following excision of the soft palate in the clamp of the sponge forceps.

Figure 19.9 Gross postmortem photograph depicting the excision of one of the soft palate “tags.” The tag is grasped with an Allis tissue forceps and is excised with scissors.

Figure 19.10 Gross postmortem photograph depicting completion of the staphylectomy procedure. Rostral is at the bottom of the photograph and caudal is toward the top of the photograph.

Chapter 20

Figure 20.1 Intraoperative image showing the ventral aspect of the throatlatch area after skin incision and separation of the sternohyoideus muscle. C, cricoid cartilage; T, ventral aspect of the rostral aspect of the thyroid cartilage; B, basihyoid bone.

Figure 20.2 Intraoperative image showing the placement of the sutures into the thyroid cartilage ventral to the ST tendon. Four bites are placed to divide the forces between suture and cartilage and thus minimizing the likelihood of suture pull through.

Figure 20.3 Schematic representation of suture placement for laryngeal tie-forward sutures. (a) Ventral view: note that the dorsal suture is placed ipsilateral while the ventral suture crosses to the contralateral side. (b) Lateral view: note that both sutures are placed dorsal to the basihyoid bone to enhance the dorsal mobilization of the larynx.

Figure 20.4 Two-year-old Standardbred racehorse 1 day postoperatively. Note deviation of the epiglottis to the left associated with suture pull through from the right thyroid cartilage.

Figure 20.5 Radiograph of a 6-year-old Thoroughbred mare after laryngeal tie-forward using metal implants to reinforce the thyroid cartilage based on Rossignol's technique.

Chapter 21

Figure 23.2 Radiograph of a horse with failed tie-forward. Note the ossification at the base of the thyroid cartilage (*) is caudal to the thyrohyoid bone.

Figure 23.3 Ultrasound image obtained with an 8.5-MHz semiconvex probe showing a loose tie forward suture upon head extension in a 3-year-old Thoroughbred filly.

Figure 23.4 Ultrasonographic image obtained with an 8.5-mHz semiconvex probe showing a suture in the cricoid cartilage after laryngeal tie-forward in a 3-year-old Thoroughbred filly.

Chapter 24

Figure 24.1 Horse with enlarged lymph node in the floor of the medial compartment of the guttural pouch near the pharyngeal branch of the vagus (white arrows).

Figure 24.2 Fungal lesions over internal carotid artery in close proximity to cranial nerves IX, X, XI, XII.

Figure 24.3 Horse with persistent DDSP; notice that the soft palate is flat with no evidence of an epiglottic bulge or mass on its oral surface. This is typically seen in horses with intermittent displacement as well.

Figure 24.4 Horse with persistent displacement and an epiglottic bulge (white arrows) on its oral surface suggesting that the epiglottic cartilage is enlarged or deformed.

Figure 24.5 Horse with persistent displacement of the soft palate during a swallow after a laryngeal tie-forward. Note the epiglottic bulge underneath the soft palate.

Figure 24.6 Horse with persistent DDSP after laryngeal tie-forward. The horse is being prepared for a laser staphylectomy. Note the three “dots” placed on the soft palate prior to resection with the diode laser. These “dots” serve as a guide for the soft palate resection. The bronchoesophageal grasping forceps are in the upper left of the photograph and the diode laser fiber is contacting the soft palate.

Chapter 25

Figure 25.1 A vertical cut through the caudal part of the septum directly below the trephine places the septal stump where swelling from edema, granulation tissue, and fibrosis (broken line) could occlude the nasal passage by impinging on the adjacent conchae (a). If the caudal cut is directed as far caudally as possible on the septum (b), then the swelling in the septal stump (broken line) will be in a wide part of the nasal passage and will not impinge on adjacent structures.

Figure 25.2 Resin cast of the left nasal passage of a horse between the septum and the bony components of the nasal passages showing the septal surface. Note that the caudal part of the floor of the nasal passage declines ventrally at the caudal end (below white line).

Figure 25.3 Introduction of wire x through one nasal passage and exiting through the mouth (a,b) after manual retrieval around the soft palate. Wire y is introduced the same way through the contralateral nostril and the two ends outside the mouth are spliced together with adhesive tape (c). The nasal portion of each wire is black and the oral portion is gray in (b). Wire y is pulled in the direction of the arrow (c) to bring the splice and the other end of wire